Makoto Kobayashi
CRIEPI
1–6–1, Ohtemachi, Chiyoda-ku, Tokyo, 100–8126 JAPAN
e-mail: mkob@criepi.denken.or.jp
phone: +81 3 3201 6601
fax: +81 3 3287 2841

Hiromi Shirai
CRIEPI
2-6-1, Nagasaka, Yokosuka-shi, Kanagawa, 240-0196 JAPAN
e-mail: sira@criepi.denken.or.jp
phone: +81 468 56 2121
fax: +81 468 56 3346

Makoto Nunokawa
CRIEPI
2-6-1, Nagasaka, Yokosuka-shi, Kanagawa, 240-0196 JAPAN
E-mail: nuno@criepi.denken.or.jp
Phone: +81 468 56 2121
Fax: +81 468 56 3346

Stability of Sulfur Capacity Attributed to Zinc Sulfidation on Sorbent Containing Zinc Ferrite–Silica Composite Powder in Pressurized Coal Gas.

Keywords: **Desulfurization, Thermogravimetry, in Situ XRD, Sulfidation Mechanism**

Introduction

A regenerable desulfurization sorbent for hot gas cleaning that is able to reduce concentration of sulfur compounds below the part-per-million level requires zinc-containing oxides as a reactant. Zinc ferrite (Grindley 1987, Focht et al. 1988 and 1989), zinc titanate (Lew et al. 1992), and other double oxides (Patriic et al. 1989) have been investigated for many years, because these oxides have thermodynamically favorable properties for sulfur reduction. Zinc ferrite–silicon dioxide composite powder (Kobayashi et al. 1997) has been investigated as a candidate material for a high-temperature fuel gas desulfurization sorbent. Sulfur removal with the double oxide was achieved with sulfidation reaction of both zinc and iron. When the sorbent is used in multiple desulfurization cycles, which consist of desulfurization, regeneration, and reduction, the sulfur capacity of the sorbent decreased as a result of sulfate formation (Kobayashi et al. 1996). Although the tendencies for sulfate formation of zinc and iron might differ under specific reaction conditions, no suitable methodology is available to distinguish the amount of sulfate in terms of the kind of metal. Because the sulfur removal performance at lower concentrations of around the part-per-million level depends on zinc, sulfur capacity of zinc portion is essential to maintain the performance. Thus, it is very important to distinguish the capacity decrease due to zinc sulfate production. It might be effective to reveal reaction schemes of zinc and iron during sulfidation to compare the reactivity of the two metals. Reaction schemes for sulfidation were estimated indirectly from thermodynamic calculations (Kobayashi et al. 1996) and thermogravimetry (Kobayashi et al.

1994). The estimation was based on the stoichiometry of the sulfidation products: zinc and iron produce sulfides with a definite ratio of metal to sulfur, i.e., ZnS and FeS. This assumption is also used to calculate the sulfur capacity of the sorbent in a fixed-bed reactor test; the amount of sulfur absorbed by the sorbent was compared to the value assumed by stoichiometry. As the capacity expresses the sum of the sulfur reacted with zinc and iron, we call it the total sulfur capacity. Our recent study (Kobayashi et al. 2000 and 2002) revealed the actual sulfidation scheme of zinc ferrite by complementary analysis of in situ X-ray diffraction and Mössbauer spectroscopy. The most significant findings was that stoichiometric zinc sulfide was produced solely at lower concentrations below the thermodynamic boundary condition. It is possible that sulfidation tests at lower concentrations enable the sulfur capacity due to zinc sulfidation to be estimated.

Objectives

This paper describes an attempt to divide the total sulfur capacity into its contribution from zinc and iron using a pressurized-type thermobalance. The methodology to estimate the sulfur capacities corresponding to zinc and iron was applied to evaluate the variation in performance during multiple-cycle desulfurization. Primary objective of this paper is providing information on the stability of zinc-related sulfur capacity, which is essentially important to the sulfur removal performance at the concentration of the part-per-million level.

Approach

Zinc ferrite–silica composite powder was prepared by the urea-precipitation method. Sulfidation scheme of zinc ferrite in the powder was determined by in situ X-ray diffraction. Thermogravimetry at pressurized condition determined the sulfur capacities of the fresh sorbent based on the sulfidation scheme; sulfidation at high and low concentrations of hydrogen sulfide made possible to determine both the capacities. This method was applied to evaluate each sulfur capacities of zinc and iron for the sorbent that was spent during multiple-cycle desulfurization. The change in the capacity attributed to zinc was estimated by extrapolating the observed capacity change along the 20 repetitions of desulfurization cycles.

Project Description

Specimen of Sorbent Containing Zinc Ferrite–Silica Composite Powder. Zinc ferrite–silica composite powder was prepared by the urea-precipitation method described in our previous work (Kobayashi et al., 1996). The atomic ratio of the metallic elements Zn, Fe, and Si in the prepared powder was 1.0:2.0:2.0. The obtained powder was ground in an agate mortar and pestle. The composite powder was subjected to a series of reduction and sulfidation steps in an in situ XRD instrument (MAC Science Co., Ltd., MXP18VAHF22-

SRA) to verify the reaction schemes for the zinc ferrite portion of the composite powder in a simulated coal gas environment.

The pelletized desulfurization sorbents was prepared from a mixture of the composite powder and tetragonal titanium dioxide as the supporting material. The composite powder was mixed with the titanium dioxide at the specific weight ratio $ZnFe_2O_4$–SiO_2/TiO_2 = 3:7. The mixture was pelletized with an extruder into a cylindrical shape of 3-mm diameter. The pellets were dried and calcined at 700 °C. The details of the preparation procedures for the composite powder and pelletized sorbent are the same as described in our previous work (Kobayashi et al., 1996 and 1997). The extruded pellets had various lengths and shapes. Specimens for further tests in a fixed-bed reactor and thermobalance were prepared by crushing the pellet and sieving it to 1.0–1.4 mm in diameter.

In Situ XRD Analysis. The composite powder was subjected to reduction and sulfidation in an in situ XRD instrument whose details were described in a previous paper (Kobayashi et al., 2000). The main components around the optical system of the instruments are shown schematically in Figure 1. The instrument is equipped with a high-temperature sample stage for humid, corrosive gas. Throughout our experiments, Cu Kα radiation (λ = 1.54056 Å) with an output of 12 kW (40 kV × 300 mA) was used to obtain diffraction patterns. Diffraction measurements were made for diffraction angles, 2θ, between 20 and 56° with an average scanning speed of 0.6°/min. Thus, a measurement was completed every 60-min intervals. Because the distinctive peaks identifying the product phases were distributed between 29 and 44°, the maximum time lag that emerged in the range of angle was only 25 min. Sample preparation on a specially manufactured quartz cell was also described in a previous work (Kobayashi et al., 2000). The temperature applied to the sample stage was 450–550 °C. Reduction and sulfidation were performed with a simulated coal gas composition of a dry coal fed and air-blown-type gasifier as shown in Table 1. Because the reaction gas was prepared by mixing each component gas supplied by mass flow controllers, the concentration of hydrogen sulfide was easily controlled to desired value. Reduction tests were performed in the simulated coal gas without hydrogen sulfide. Sulfidation reactions were performed in the gas containing hydrogen sulfide whose concentration was adjusted between 80 and 500 ppm. This concentration range was chosen from the thermodynamic aspects and experimental restrictions described precisely in our previous work (Kobayashi et al., 2000).

Multiple Desulfurization Cycles in a Fixed-Bed Reactor. Sulfidation cycle tests of the sieved sorbents were carried out in our apparatus with a fixed-bed reactor (37.5 mm i.d.) under pressurized conditions. A continuous sulfur concentration analyzer (Yanaco Ohgi, TSA-1001) equipped with a Flame Photometric Detector (FPD) to measure concentrations of sulfur compounds up to 2 vol % in desulfurization was used to analyze the exit gas stream.

The data were used to calculate the sulfur balance of the sorbents. An oxygen analyzer (Servomex, Ltd., oxygen analyzer 540A) was used to determine the termination of the oxidation reactions. The reaction conditions are summarized in Table 2. The sieved pellets were packed into the fixed-bed reactor and heated to a predetermined temperature in a stream of nitrogen gas. Sulfidation was performed by introducing a gas mixture that simulates coal gas produced in a dry coal fed, air-blown coal gasifier. Sulfidation was continued until complete breakthrough occurred. The definition of complete breakthrough is when the sulfur concentration at the reactor outlet levels off at a concentration over 90% of the inlet sulfur concentration. The total sulfur capacity of the sorbent was determined by material balance of sulfur compounds at the inlet and outlet of the sorbent bed during sulfidation. Regeneration was carried out in oxygen mixed with nitrogen, as shown in Table 2, until breakthrough of oxygen. A reduction step followed regeneration to complete the removal of sulfur from the sorbent bed. Simulated coal gas without sulfur compounds was also used in reduction (Table 2). Sulfur elution from the reactor outlet during regeneration and reduction was analyzed to evaluate the regenerability of the sorbent.

Pressurized-Type Thermobalance. Thermogravimetry was carried out on a pressurized-type thermobalance designed for humid corrosive gas (ATI Chan, TG-151). The obtained data were analyzed to distinguish the sulfur capacity corresponding to zinc sulfidation from the total sulfur capacity. The balance mechanism and sample furnace were used as supplied by ATI Cahn, although the humid gas supplying unit and balance elevation mechanism were designed and customized by Santeck Co., Ltd., for the specific test. The modification enabled precision measurements under pressurized gas conditions. The resolution of the balance mechanism is 1 μg at the maximum sample loading of 10 g. A sorbent specimen of typically 100 mg was loaded on the balance with a sample basket made of quartz. The sample furnace was operated at 450 or 550 °C after the gas stream was pressurized up to 0.98 MPa with nitrogen. When the weight indication was stabilized, the inert gas was changed to reduction gas. After the reduction step was continued for 1 h, the test proceeded to the sulfidation step. The gas composition for the reduction and succeeding sulfidation steps are summarized in Table 1. It was judged that termination of the sulfidation reaction occurred when the average weight change for a 10-min interval fell below 1% of the cumulative weight change. The test results were analyzed on the basis of the dry sample weight after sulfidation, because the loaded sample weight included humidity.

Results

Reaction Schemes of Reduction and Sulfidation of Zinc Ferrite–Silica Composite Powder. Figures 2 and 3 display diffraction patterns that were obtained by in situ XRD measurements of sulfidation of the composite powder in the simulated coal gas with different H_2S concentrations at 450 °C. The first measurement shown in both figures was performed in

the gas without H_2S for 1 h, which ensures a reductive environment around the sample. Hydrogen sulfide was then introduced at 500 and 80 ppm. During sulfidation at the high H_2S concentration, sulfides of both zinc and iron were produced; the sulfidation products were wurtzite, zinc blende, cubic iron sulfide, and pyrrhotite. Iron sulfides were not produced at the H_2S concentration of 80 ppm; zinc sulfides (wurtzite and zinc blende) were confirmed by the XRD diffraction patterns as shown in Figure 3. After 20 h of sulfidation, the spinel structure remained, which is most plausibly assigned to zinc-dislocated franklinite. The same sulfidation products were identified at the reaction temperature of 550 °C, but an acceleration of the sulfidation rate was observed. These observation was essentially same as that obtained for pure zinc ferrite of which the detail of reaction scheme was precisely revealed by in situ XRD and Mössbauer spectroscopy in our previous work (Kobayashi et al. 2000 and 2002). Thus, the sulfidation scheme of the composite powder was verified to be same as hat determined for pure zinc ferrite as summarized in Figure 4, which is applicable to an analysis of the weight variation data obtained with thermobalance.

Sulfidation at Dual Sulfur Concentration for the Determination of Contribution to the Sulfur Capacity of Zinc and Iron. The sulfidation scheme, which was verified for the composite powder in the previous section, should be identical to the reaction schemes of desulfurization sorbents containing the same composite powder. Supporting materials in the sorbent are considered to be inert in the reaction, but a variation in the physical properties might actually affect the reaction rate. Thus, we applied the reaction schemes displayed in Figure 4 to an analysis of the thermobalance tests of the sulfidation of the sorbent. To confirm the validity of the analyses, we performed sulfidation tests of fresh sorbent. A pressurized-type thermobalance was used to determine the sulfur capacities of zinc and iron separately. We tried to distinguish the contributions of zinc and iron to sulfidation by varying the H_2S concentration so that the sulfidation conditions were situated across the phase boundary between iron oxide and its sulfide. Because both zinc and iron were considered to be sulfurized at a H_2S concentration of 1 vol %, the total sulfur capacity should be determined by thermogravimetry at the high H_2S concentration. The weight increase during sulfidation of fresh sorbent observed by the pressurized thermobalance is displayed in Figure 5. The total sulfur capacity of fresh sorbent was calculated as 2.48 mmol/g. This value indicates the number of moles of sulfur captured per unit weight of fresh sorbent. Because the sorbent weight varies upon reduction and sulfidation, the specific sulfur capacity was calculated in terms of the weight of unreacted fresh sorbent. The calculated value was 99.6 % of the capacity determined by assuming stoichiometric sulfidation of zinc and iron. The error in determining the total sulfur capacity of fresh sorbent was reasonably small; thus, further discussion will assume this result. A sulfidation test at the lower sulfur concentration (80 ppm) was conducted to obtain an estimated zinc-related sulfur capacity of fresh sorbent. The thermobalance test results are displayed in Figure 6. The capacity was estimated as 0.72

mmol/g by assuming sulfidation products of ZnS and Fe_3O_4. This value was 86.2% of the value calculated by assuming complete sulfidation of zinc (0.83 mmol/g). The difference between the estimated value and the value calculated by this method indicates the existence of unreacted zinc. Although the value obtained by our method might be smaller than the amount of zinc that is available to be sulfurized at sufficiently high sulfur concentration, it is practically correct as the amount of reactive zinc at the low sulfur concentration. Thus, the estimated sulfur capacity for zinc sulfidation is important in the practical estimation of the deep-desulfurization performance of the sorbent.

This dual H_2S concentration test of sulfidation was applied to evaluate the sulfur capacity of the sorbent used in multiple desulfurization cycles. We have to define the assumptions for analyzing the thermogravimetric results for such spent sorbents. The reduction of the sulfate produced in the oxidative regeneration step give rise to sulfides; both zinc sulfate and iron sulfate are reduced to form ZnS and FeS, respectively. Alhough chemical forms of oxides produced in the oxidation step are not known precisely, the oxidation numbers of zinc and iron are uniquely defined to +2 and +3, respectively; $ZnFe_2O_4$, ZnO, and Fe_2O_3 are the expected products. Thus, the ratio of the metals to oxygen are unique for such oxides. We can assume that hematite, Fe_2O_3, is reduced to magnetite, Fe_3O_4, during reduction. In the next section, we will derive a procedure for estimating the sulfur capacities of spent sorbents by applying these assumptions and the reaction schemes.

Procedure for Sulfur Capacity Analysis. Because the sorbent used in multiple-cycle desulfurization retained residual sulfur, proper data analysis of the thermobalance tests is required to calculate accurate sulfur capacities. The procedure for analyzing the thermobalance data is derived in this section to determine the sulfur capacities related to zinc and iron from sulfidation tests at dual concentrations.

The zinc ferrite–silica composite powder has three metallic elements, Zn, Fe, and Si, with a 1.0:2.0:2.0 molar ratio. The weight ratio of zinc ferrite to silica in the composite powder is 2:1. Because the sorbent has a $ZnFe_2O_4$–SiO_2-to-TiO_2 weight ratio of 3:7, the weight fraction of zinc ferrite in the sorbent is 0.2. The remaining portion is silica and titania, whose weight fraction is 0.8. When one takes a unit weight of the sorbent, it contains 0.2 g of $ZnFe_2O_4$. It was assumed that sulfidation at 1 vol % of H_2S produces stoichiometric sulfides, ZnS and FeS. This assumption allows the amounts of zinc and iron in the sorbent to be estimated from the weight of the sample that was completely sulfurized at the higher sulfur concentration. If we describe the composition of the stoichiometric sulfide as $ZnFe_2S_3$, its weight is expressed as

$$w_{ZFS} = 0.2m_{ZFS} / m_{ZF} \quad \text{---------- (1)}$$

where m_{ZFS} and m_{ZF} denote the molar weights of $ZnFe_2S_3$ and $ZnFe_2O_4$, respectively. Thus, the weight fraction of $ZnFe_2S_3$ in the sorbent is expressed as

$$\chi_{ZFS} = 0.2m_{ZFS} / (0.2m_{ZFS} + 0.8m_{ZF}) \quad \text{---------- (2)}$$

Thus, the number of moles of $ZnFe_2S_3$, n_{ZFS}, is derived by introducing the weight of sorbent after complete sulfidation, W_{CS}, as in eq 3. The law of conservation of mass guarantees that n_{ZFS} equal the number of moles of zinc ferrite in fresh sorbent, n_{ZF}

$$n_{ZFS} = n_{ZF} = W_{CS}\chi_{ZFS}/m_{ZFS} \quad (3)$$

Multiplication of n_{ZF} by the difference between the molar weights of $ZnFe_2S_3$ and $ZnFe_2O_4$ gives the expected weight increase during complete sulfidation, ΔW_{CS}^{MAX}, as shown in eq 4

$$\Delta W_{CS}^{MAX} = n_{ZF}(m_{ZFS} - m_{ZF})$$
$$= n_{ZF}(3m_S - 4m_O) \quad (4)$$

where m_S and m_O denote the atomic weights of sulfur and oxygen, respectively. One can derive the estimated weight of fresh sorbent as

$$W_{ZF} = W_{CS} - \Delta W_{CS}^{MAX} \quad (5)$$

If one assumes that the observed weight increase during sulfidation, ΔW_{CS}^{EXP}, is proportional to the conversion of the sulfidation reaction of both zinc and iron, then the overall conversion can be espressed as

$$X_{ZF} = \Delta W_{CS}^{EXP}/\Delta W_{CS}^{MAX} \quad (6)$$

The conversion corresponds to the total sulfur capacity, ρ_{ZF}, which is given by

$$\rho_{ZF} = 3X_{ZF}n_{ZF}/W_{ZF} \quad (7)$$

Because sulfidation at 80 ppm of H_2S does not produce iron sulfides, the weight of complete sulfidation was estimated from the weight ratio of loaded samples as expressed in eq 8

$$W_{CS}^{EST} = W_{CS}\, M_{LS}/M_{CS} \quad (8)$$

where M_{LS} and M_{CS} express the loaded sample weights for sulfidation tests at the low and high concentrations, respectively. Then, the estimated unsulfurized sample and maximum weight increase during zinc sulfidation are expressed by eqs 9 and 10, respectively

$$W_{ZF}^{*} = W_{CS}^{EST} - \Delta W_{CS}^{MAX} \quad (9)$$

where ΔW_{CS}^{MAX} should be recalculated by applying eqs 3 and 4 to the sample for low-concentration sulfidation

$$\Delta W_{LS}^{MAX} = n_{ZF}(m_{ZSF} - m_{ZF})$$
$$= n_{ZF}(m_S - 4m_O/3) \quad (10)$$

If one measures the actual weight increase during zinc sulfidation, the zinc-related sulfur capacity can be calculated by eq 11. The conversion gives the zinc-related sulfur capacity, ρ_Z, as shown in eq 12

$$X_Z = \Delta W_{LS}^{EXP}/\Delta W_{LS}^{MAX} \quad (11)$$

$$\rho_Z = X_Z n_{ZF}/W_{ZF}^{*} \quad (12)$$

In the next section, we adopt the above formulas to determine the sulfur capacity of sorbent that experienced multiple desulfurization cycles.

Change in Sulfur Capacity Related to Zinc During Multiple Desulfurization Cycles. The total sulfur capacity of the sorbent was measured during multiple desulfurization cycles in the same apparatus as in our previous work (Kobayashi et al., 1996). The sulfur capacity was

determined by an analysis of the complete breakthrough curves obtained with the pressurized fixed-bed reactor. The reaction conditions shown in Table 2 were applied to the test. The condition is identical to those in Table 1 under which the thermobalance tests were conducted. The reproducibility of the sulfur capacity change was confirmed up to the 12th cycle, where we observed a relatively large decrease of the capacity. The decreasing tendency was the same as found in the 20-cycle test within experimental error. Therefore, we chose samples of spent sorbent during multiple-cycle desulfurization from the tests of up to 20 cycles. The test results for fixed-bed sulfidation are displayed by filled squares in Figure 7. Although the capacity decreased rather rapidly during the initial few cycles, the tendency slowed with repetition up to 20 cycles. The decreasing sulfur capacity is caused mainly by residual sulfur due to sulfate formation (Kobayashi et al., 1996). The ratio of zinc sulfate to iron sulfate is not clear, because it is difficult to distinguish zinc sulfate from iron sulfate quantitatively by the usual chemical analyses. When zinc sulfate is selectively produced during regeneration, the sulfur removal performance at lower concentrations might be diminished. It is not practical to determine the zinc-related sulfur capacity with a fixed-bed reactor, because sulfidation at low H_2S concentration takes a long time; the reaction time required to complete sulfidation at 80 ppm can typically be 125 times longer than that at 1 vol %. Thus, we tried to determine the change in zinc-related sulfur capacity during desulfurization cycles by applying the dual-H_2S-concentration method with a pressurized thermobalance. The samples were spent sorbents taken from repeated desulfurization cycle tests in a fixed-bed reactor; a series of spent sorbents after the initial few cycles and after 20 cycles were subjected to the thermobalance test to determine their zinc-related sulfur capacities as well as their total sulfur capacities. The measured sulfur capacity data are plotted in Figure 7. Because each sulfidation test in thermobalance was counted as one cycle, the results are plotted as a function of the cycle of the sample plus 1. The total sulfur capacity analyzed by thermogravimetry is able to reproduce the data obtained in the fixed-bed reactor. Thermobalance tests at lower sulfur concentration (80 ppm) were performed for the same series of samples. The analyzed zinc-related sulfur capacity was subtracted from the total sulfur capacity to calculate the iron-related sulfur capacity. The calculated values are plotted in Figure 7 as filled triangles. The iron-related sulfur capacity was stable during the cycles. At the 21st cycle, the zinc-related sulfur capacity decreased to about 50% of its initial value, whereas the iron-related sulfur capacity maintained 91% of its initial value. This indicates that the decrease in the total sulfur capacity was caused by residual sulfur due to zinc sulfate.

Zinc ferrite–silica composite powder was subjected to the series of reduction and sulfidation tests performed at mainly 450 °C in simulated coal gas environment. Products of reduction and succeeding sulfidation were determined by the in situ X-ray diffraction analyses revealed that ZnS and FeS were produced at H_2S concentration of 1 vol %, whereas only zinc sulfides were detected at 80 ppm. It was reasonably explained that iron component remained as zinc

bearing magnetite or pure magnetite, which were also observed during sulfidation of pure zinc ferrite by Mössbauer spectroscopy. These reaction products of the composite powder confirmed that the reaction scheme was essentially the same as that of pure zinc ferrite sulfurized at 550 °C in the same gas composition. Pressurized thermobalance was operated to determine sulfur capacity of zinc and iron separately by performing sulfidation at H_2S concentration of 80 ppm and 1 vol %. Total sulfur capacity measured for the fresh sorbent was consistent with the capacity that was calculated from the complete breakthrough curves obtained by fixed bed reactor test. Sulfur capacity due to zinc-sulfidation of fresh sorbent measured by the method was around 86% of the value calculated by assuming complete sulfidation of zinc element. This method was applied to analyze the change in the zinc-related sulfur capacity of sorbent samples that experienced multiple desulfurization cycles up to 20 times. At the end of the cycles, the zinc-related sulfur capacity had fallen to about 50% of its initial value, whereas the sulfur capacity due to iron sulfidation maintained 91% of its initial value. This indicates that the decrease in the total sulfur capacity mainly results from the residual sulfur due to zinc sulfate production during regeneration. Extrapolation of experimental data for initial 20 cycles of desulfurization suggested that zinc sulfur capacity would level off at around 40% of its initial value within 50 cycles.

Application

A method to measure sulfur attributed to zinc sulfidation on the zinc ferrite containing sorbent was established. The method was applicable to evaluate the stability of the zinc-related sulfur capacity during the multiple desulfurization cycle up to 20 times. Tendency of decrease of the zinc-related sulfur capacity in further cycles was estimated by extrapolating the experimental data; the capacity would likely to be leveled off at about 40% of its initial value. Desulfurization tests up to 50 repetitions are required to confirm the estimation. Examination on the effect of the decrease in the sulfur capacity on the sulfur removal performance at the low sulfur concentration is also task of the future investigation.

Conclusion

Thermogravimetric analyses based on the sulfidation scheme determined each the sulfur absorbing capacities of zinc and iron in the sorbent containing zinc ferrite–silica composite powder. The method was applied to sorbent samples that experienced multiple desulfurization cycles in pressurized coal gas at 450 °C. After repetition of 20 sulfidation-cycles, zinc-related sulfur capacity had fallen to about 50% of its initial value, whereas the sulfur capacity due to iron-sulfidation maintained 91% of its initial value. Extrapolation of the experimental data indicated that the capacity of zinc would level off at around 40% of its initial value within 50 desulfurization cycles. This suggests that the sulfidation performance at the low sulfur concentration would be maintained for successive sulfidation cycles.

Reference

Grindley, T., 1987. Sidestream zinc ferrite regeneration testing. In *Proceedings of the Seventh Annual Gasification and Gas Stream Cleanup Systems Contractors Review Meeting*; DOE/METC-87/6079; U.S. Department of Energy, U.S. Government Printing Office: Washington, DC, Vol. 2: pp 567–578.

Focht, G. D., Ranade, P. V., Harrison, D. P., 1988, High-Temperature Desulfurization Using Zinc Ferrite: Reduction And Sulfidation Kinetics. *Chem. Eng. Sci.* 43 (11): 3005–3013.

Focht, G. D., Ranade, P. V., Harrison, D. P., 1989. High-Temperature Desulfurization Using Zinc Ferrite: Regeneration Kinetics and Multicycle Testing. *Chem. Eng. Sci.* 44 (12): 2919–2926.

Kobayashi, M., Shirai, H., Nunokawa, M., 1997. Investigation on Desulfurization Performance and Pore Structure of Sorbents Containing Zinc Ferrite. *Energy Fuels* 11 (4): 887–896.

Kobayashi, M., Nunokawa, M., Shirai, H., 1996. Development of regenerable desulfurization sorbent for coal gas sulfur removal below ppm level. In *High Temperature Gas Cleaning*; Schmidt, E., Gäng, P., Pilz, T., Dittler, A., Eds.; Univasität Karlsruhe: Karlsruhe, Germany: pp 618–629.

Kobayashi, M., Nunokawa, M., Shirai, H., Watanabe, M., 1994. *Activation of Desulfurization Performance of Zinc Ferrite Sorbent for Use in High Temperature Sulfur Removal of Coal Derived Gas for Application to Molten Carbonate Fuel Cell Power Plant*; CRIEPI Report EW93005; Central Research Institute of Electric Power Industry: Yokosuka, Japan: pp 1–44.

Kobayashi, M., Shirai, H., Nunokawa, M., 2000. Elucidation of Sulfidation Mechanisms of Zinc Ferrite in a Reductive Gas Environment by in Situ X-ray Diffraction Analysis and Mössbauer Spectroscopy. *Ind. Eng. Chem. Res.* 39 (6): 1934–1943.

Kobayashi, M., Shirai, H., Nunokawa, M., 2002. High-Temperature Sulfidation Behavior of Reduced Zinc Ferrite in Simulated Coal Gas Revealed by in Situ X-ray Diffraction Analysis and Mössbauer Spectroscopy. *Energy Fuels* 16 (3): 601–607.

Lew, S.; Sarofim, A. F.; Flytzani-Stephanopoulos, M., 1992. Sulfidation of Zinc Titanate and Zinc Oxide Solids. *Ind. Eng. Chem. Res.* 31(8): 1890–1899.

Patrick, V.; Gavalas, G. R.; Flytzani-Stephanopoulos, M.; Jothimurugesan, K., 1989. High-temperature sulfidation—regeneration of CuO—Al_2O_3 sorbents. *Ind. Eng. Chem. Res.* 28(7), 931–940.

Figures and Tables

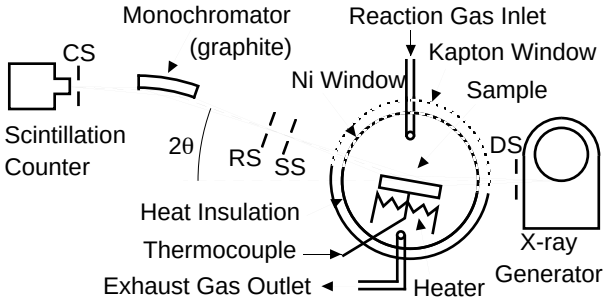

Figure 1 Optical geometry and reactor schematic of the in situ XRD spectrometer.

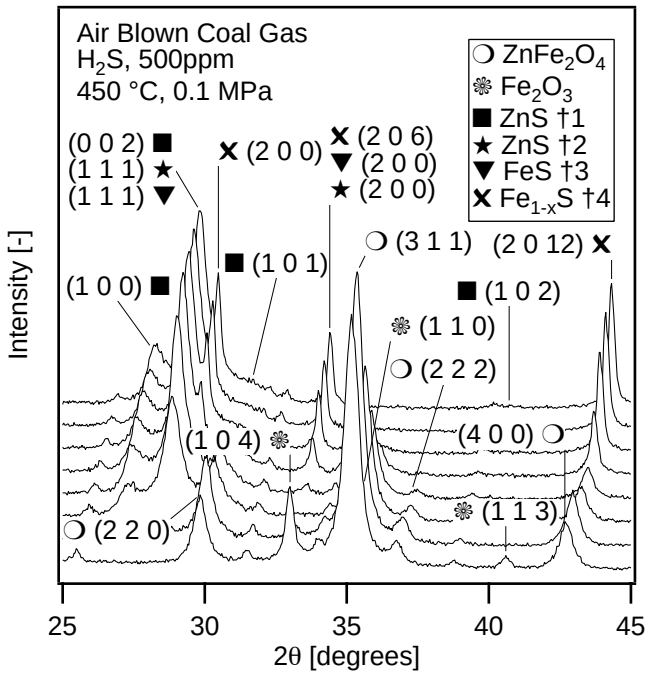

Figure 2. Variation of X-ray diffraction pattern of pure zinc ferrite-silica composite particle during sulfidation in coal gas environment with 500 ppm H_2S concentration at 450 °C (†1, wurtzite; †2, zinc blend; †3, cubic; †4, pyrrhotite-6T).

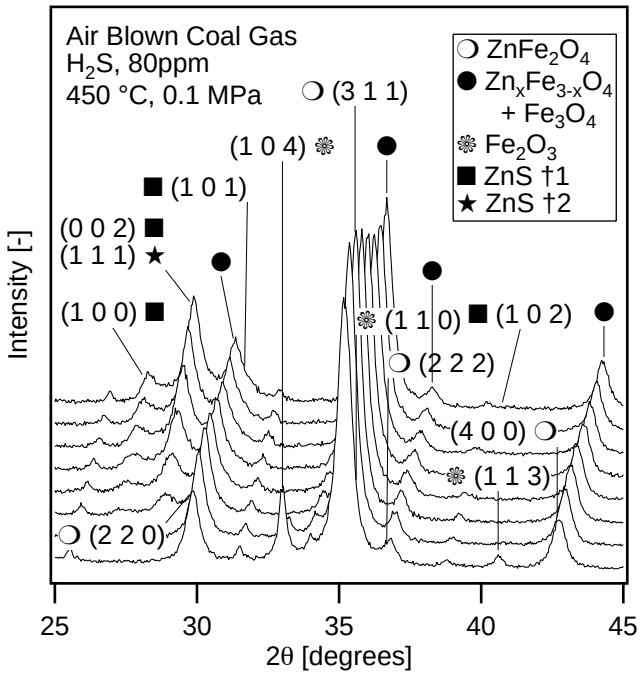

Figure 3. Variation of X-ray diffraction pattern of pure zinc ferrite-silica composite particle during sulfidation in coal gas environment with 80 ppm H_2S concentration at 450 °C (†1, wurtzite; †2, zinc blend).

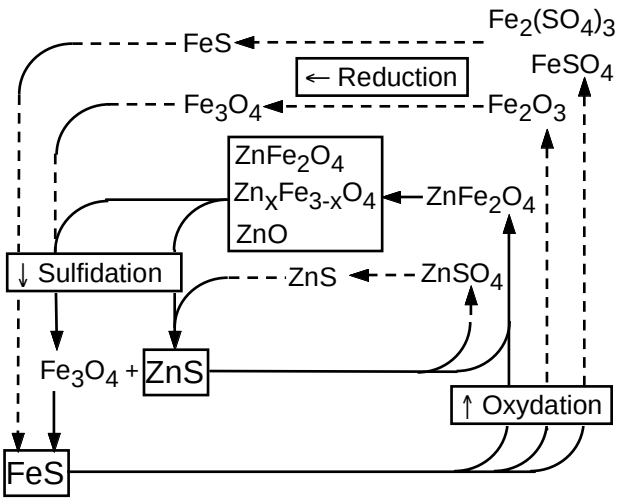

Figure 4. Reaction schemes on reduction and sulfidation of pure zinc ferrite-silica composite particle in coal gas environment at 450 °C.

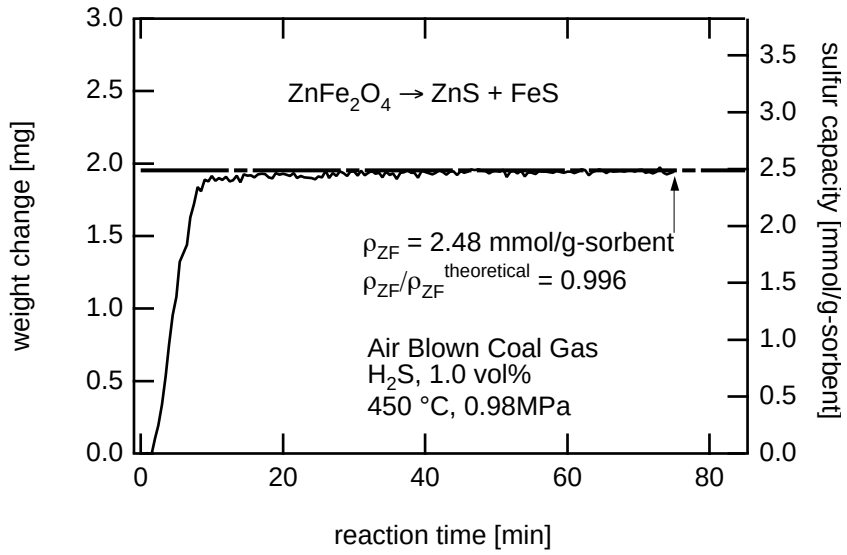

Figure 5. Sulfidation reaction on desulfurization sorbent containing zinc ferrite–silica composite powder at high H_2S concentration and calculated sulfur capacity.

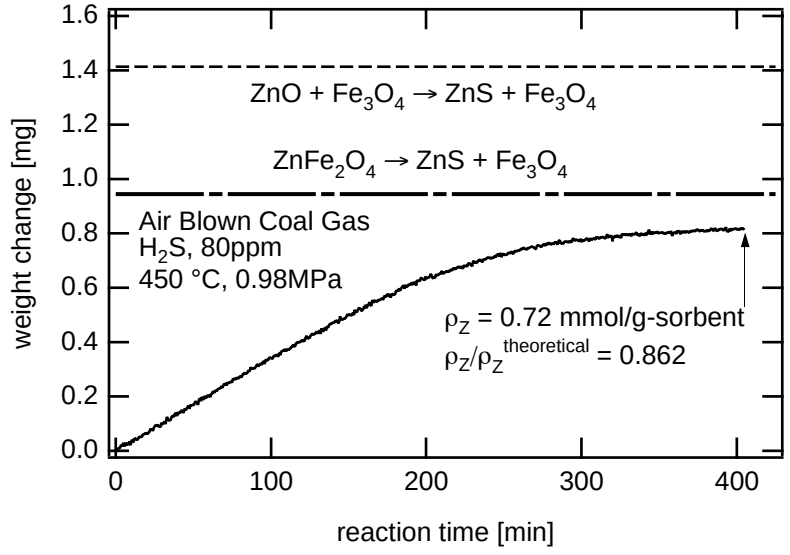

Figure 6. Sulfidation reaction on desulfurization sorbent containing zinc ferrite–silica composite powder at low H_2S concentration and calculated sulfur capacity related to zinc sulfidation.

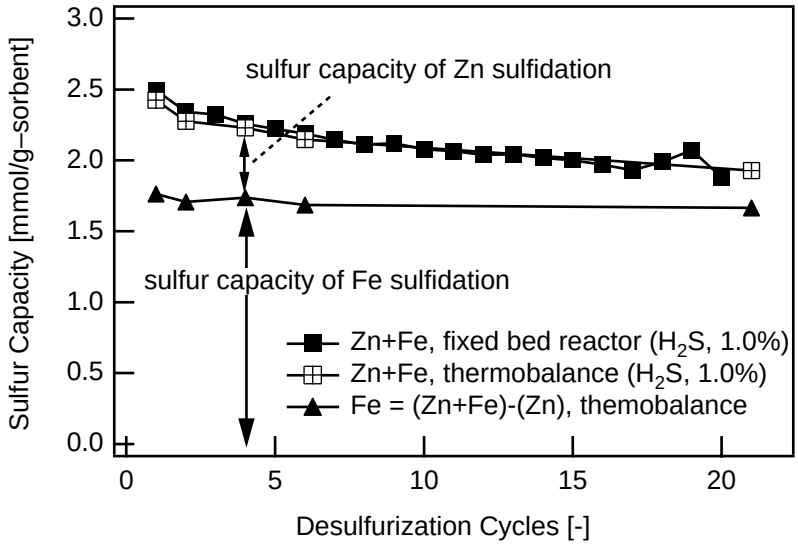

Figure 7. Sulfur capacities of desulfurization sorbent containing zinc ferrite–silica composite powder during multiple desulfurization cycles.

Table 1. Conditions for Reduction and Sulfidation Tests

	in situ XRD	TGA
temp, °C	450–550	450
pressure, MPa	0.10	0.98
gas composition, vol%	CO, 20; CO_2, 5; H_2, 8; H_2O, 5; N_2, balance	CO, 20; CO_2, 5; H_2, 8; H_2O, 5; N_2, balance
flow rate, cm^3/min (25 °C, 0.1 MPa)	500	500
H_2S conc[a]	0, 80–500 ppm	0, 80–500 ppm, 1%
sample wt., g	0.1	0.06–0.10

[a] Reduction was performed in the reaction gas with H_2S concentration of 0 ppm.

Table 2. Reaction Conditions for the Desulfurization Cycle Test in a Pressurized Fixed-Bed Reactor

	reduction	sulfidation	regeneration
temp, °C	450	450	450
pressure, MPa	0.98	0.98	0.98
gas composition, vol%			
CO	20.0	20.0	–
CO_2	5.0	5.0	–
H_2	8.0	8.0	–
H_2O	5.0	5.0	–
H_2S	0.0	1.0	–
O_2	–	–	1.5
N_2	balance	balance	balance
flow rate, cm^3/min (25 °C, 0.1 MPa)	1100	3300	3700
sample weight, g	60	60	60